

# RSC Advances



This is an *Accepted Manuscript*, which has been through the Royal Society of Chemistry peer review process and has been accepted for publication.

*Accepted Manuscripts* are published online shortly after acceptance, before technical editing, formatting and proof reading. Using this free service, authors can make their results available to the community, in citable form, before we publish the edited article. This *Accepted Manuscript* will be replaced by the edited, formatted and paginated article as soon as this is available.

You can find more information about *Accepted Manuscripts* in the [Information for Authors](#).

Please note that technical editing may introduce minor changes to the text and/or graphics, which may alter content. The journal's standard [Terms & Conditions](#) and the [Ethical guidelines](#) still apply. In no event shall the Royal Society of Chemistry be held responsible for any errors or omissions in this *Accepted Manuscript* or any consequences arising from the use of any information it contains.

## Organo-metal perovskite based solar cells: sensitized versus planar architecture

Shany Gamliel, Lioz Etgar\*

The Hebrew University of Jerusalem, Institute of Chemistry, Casali Center for Applied Chemistry, Israel

\*E-mail: [lnoz.etgar@mail.huji.ac.il](mailto:lnoz.etgar@mail.huji.ac.il)

### Abstract

Organo-metal halide perovskite is composed of ABX<sub>3</sub> structure in which A represents a cation, B a divalent metal cation and X halide. The organo-metal perovskite shows very good potential to be used as a light harvester in the solar cell due to its direct band gap, large absorption coefficient, high carrier mobility and good stability. However, there is an important question in the photovoltaic field regarding the more advantageous architecture for perovskite based solar cells. Several studies showed sensitized perovskite solar cells achieving high performance, while high efficiency was also observed with planar architecture. Consequently, it is still an open question regarding which operation mechanism and which architecture offers better results. This review describes both architectures, based on studies in the field. In the case of sensitized structure, there are more difficulties in pore filling, naturally more recombination, and the possibility to use thicker metal oxide films. In the planar structure, thin metal oxide films are used, less recombination was observed and there are no infiltration problems. Both architectures exhibit long-range diffusion length and meet the demand for excellent coverage of the perovskite film.

## 1. Introduction

In recent years a breakthrough has occurred in the photovoltaic field—the use of organic-inorganic perovskite as a light harvester in solar cells. The organo-metal halide perovskite solar cell has the potential of replacing current technologies due to its simple preparation, low cost, superior optical properties and high stability. Currently, much research is devoted to this issue, and researchers from various fields are involved, including theoreticians, chemists, physicists and engineers.

The most common perovskite used for PV application is the methyl ammonium lead halide ( $\text{CH}_3\text{NH}_3\text{PbX}_3$ , X=Br, Cl, I), already proposed in 2009 as an efficient light harvester in liquid solar cells.<sup>1</sup> Since then, photovoltaic performance has increased dramatically achieving efficiency of more than 16%.<sup>2,3,4,5</sup>

The possibility to tune the optical properties of the organo-metal halide perovskite paves the way to high voltage cells. Open circuit voltage ( $V_{oc}$ ) of 1.15 V and 1.3 V using  $\text{CH}_3\text{NH}_3\text{PBr}_3$  as a light harvester with various hole transport materials has been demonstrated.<sup>6,7</sup>

It may seem obvious to consider perovskite-based solar cells as a new kind of dye sensitized solar cells (DSSC). However, several reports shed new light on high efficiency planar perovskite-based solar cells. Are perovskite-based solar cells more like sensitized solar cells, or planar heterojunction solar cells? In this review, we present research from both points of view, describing the advantages and disadvantages of sensitized perovskite solar cells and planar perovskite solar cells.

## 2. Crystal structure of organo-metal halide perovskite

One of the pioneer studies on the perovskite structure was conducted in the 1920s by Goldschmidt et al.<sup>8</sup> The crystal structure of the ideal perovskite (the 3D perovskite crystal structure) is cubic  $\text{ABX}_3$  consisting of corner sharing (BX<sub>6</sub>) octahedra with the A cation occupying 12-fold coordination site. The B cation is a divalent metal, which satisfies the charge balancing. Examples for the metal cation include:  $\text{Cu}^{2+}$ ,  $\text{Ni}^{2+}$ ,  $\text{Co}^{2+}$ ,  $\text{Fe}^{2+}$ ,  $\text{Mn}^{2+}$ ,  $\text{Cr}^{2+}$ ,  $\text{Pd}^{2+}$ ,  $\text{Cd}^{2+}$ ,  $\text{Ge}^{2+}$ ,  $\text{Sn}^{2+}$ ,  $\text{Pb}^{2+}$ ,  $\text{Eu}^{2+}$ , or  $\text{Yb}^{2+}$ . The basic structures of organo-metal perovskite are  $(\text{R-NH}_3)_2\text{MX}_4$  and  $(\text{NH}_2\text{-R-NH}_2)\text{MX}_3$ ; (X =  $\text{Cl}^-$ ,  $\text{Br}^-$ , or  $\text{I}^-$ ).<sup>9</sup>

Moreover, the organic component can consist of a bilayer or a monolayer of organic cations. The ammonium head (in the case of monoammonium) of the cation

component bonds to the halogens in one inorganic layer, and the organic group extends into the space between the inorganic layers.

The organic groups are optically inert and function as 'spacer' groups by that allowing the  $ABX_3$  lattice to be maintained; however, they have a major influence on the properties of the perovskite. The organic component tunes the binding exciton energy as it influences the dielectric constant. Currently several reports showed the replacement of the commonly used methylammonium cation by the formamidinium cation, achieving broadly tunable absorption spectra.<sup>10</sup> Additionally, by changing the halides, the optical properties of the perovskite can be tuned, achieving absorption at different wavelengths.<sup>11,41</sup>

Organo-metal halide perovskite has good potential to be used as a light harvester in the solar cell due to its direct band gap, large absorption coefficients<sup>12</sup> and high carrier mobility<sup>13,14</sup>

### 3. Sensitized perovskite based solar cells

Figure 1 describes the solar cell structure of a perovskite sensitized solar cell when the perovskite penetrates through the mesoporous metal oxide (commonly  $TiO_2$ ). In this cell structure, there is close contact between the perovskite and the metal oxide, through almost all the film thickness. This section describes several studies on perovskite solar cells based on mesoporous metal oxide.

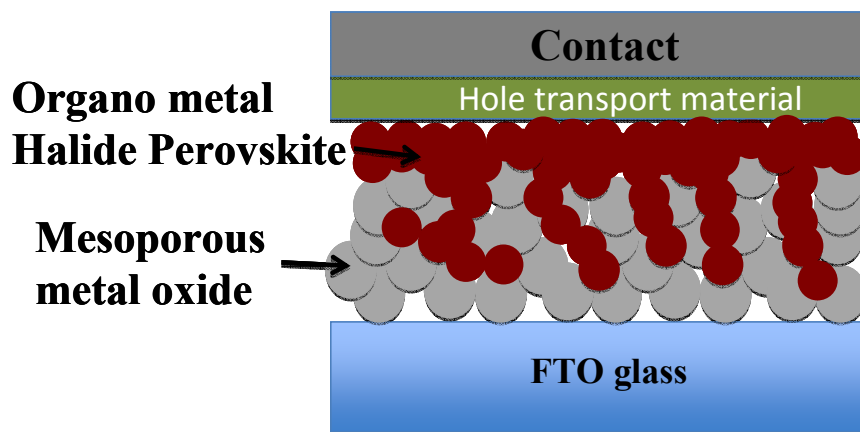


**Figure 1:** Structure of sensitized perovskite solar cell

#### Liquid electrolyte

Early work by Miyasaka et al.<sup>1</sup> reported on organo-metal nanocrystals sensitized- $TiO_2$  for solar cells. The authors used the  $CH_3NH_3PbBr_3$  and  $CH_3NH_3PbI_3$  as

sensitizers on mesoporous TiO<sub>2</sub> with liquid electrolyte achieving power conversion efficiency (PCE) of 3.18% with spectral response covering the whole visible region till 800 nm. In a later work, Park et al.<sup>15</sup> used 2–3 nm perovskite nanoparticles sensitized on 3.6 μm-thick TiO<sub>2</sub> with iodide/iodine based redox electrolyte. The solar cell efficiency was improved, achieving 6.5% with maximum external quantum efficiency (EQE) of 78.6% at 530 nm.

Zhao et al.<sup>16</sup> studied the effect of TiO<sub>2</sub> film thickness (1.8–8.3 μm) on the charge transport, recombination, and device characteristics of perovskite (CH<sub>3</sub>NH<sub>3</sub>PbI<sub>3</sub>), sensitized solar cells using iodide-based electrolytes. They showed that using electrolytes with low concentration results in relatively stable solar cells. On the other hand, polar electrolytes or higher iodide concentrations of nonpolar electrolytes achieved higher cell performances, but result in degradation or bleaching of the CH<sub>3</sub>NH<sub>3</sub>PbI<sub>3</sub>. In addition, when increasing the TiO<sub>2</sub> film thickness, although the absorption increases the overall cell performance current density ( $J_{SC}$ ), fill factor (FF), open circuit voltage ( $V_{oc}$ ), and efficiency ( $\eta$ ) were decreased.

Incident modulated voltage spectroscopy (IMVS) and intensity modulated photocurrent spectroscopy (IMPS) measurements were performed to investigate the charge transport and recombination process (figure 2). No significant effect of TiO<sub>2</sub> film thickness on electron diffusion coefficient was observed. Yet the electron recombination lifetime ( $\tau$ ) is strongly dependent on the TiO<sub>2</sub> film thickness. The decrease in electron recombination was attributed to the low electrolyte concentration (0.08M) of I<sup>-</sup> compared to the standard concentration (0.5–1M) of electrolytes. Thus, the depletion of I<sup>-</sup> enhanced within the TiO<sub>2</sub> pores with increasing TiO<sub>2</sub> film thickness; the diffusion pathway through the pores elongated with increasing TiO<sub>2</sub> film thickness. Moreover, the increases in electron recombination with increasing TiO<sub>2</sub> film thickness can be explained by increased I<sup>-</sup> deficiency with increasing TiO<sub>2</sub> film thickness.

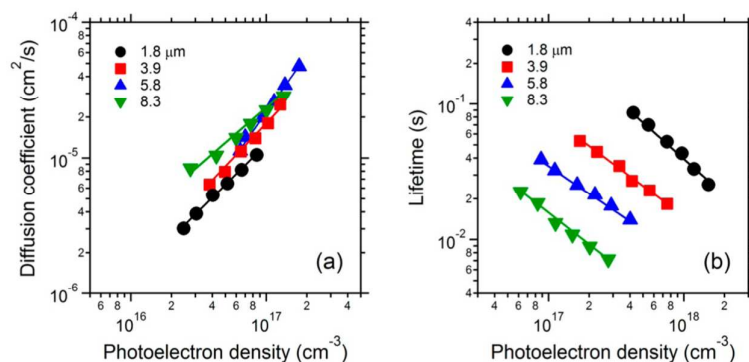


**Figure 2:** Effect of TiO<sub>2</sub> film thickness on the (a) electron diffusion coefficient and (b) recombination lifetime for (CH<sub>3</sub>NH<sub>3</sub>)PbI<sub>3</sub> sensitized cells as a function of photoelectron density. Taken from ref. 16 with permission.

### Hole transport material

Changing the liquid electrolyte to solid state hole transport material (HTM) improved the stability of the cells and enhanced their efficiency. Graetzel and Park et al.<sup>17</sup> used the methyl ammonium lead iodide CH<sub>3</sub>NH<sub>3</sub>PbI<sub>3</sub> as light harvesters deposited onto a thick mesoscopic TiO<sub>2</sub> film including solid hole conductor (spiro-MeOTAD-2,2',7,7'-tetrakis(N,N'-di-p-methoxyphenylamine)-9,9'-spirobifluorene) which was infiltrated the TiO<sub>2</sub> pores. This solid state sensitized perovskite-TiO<sub>2</sub> solar cell achieved PCE of 9.7% with J<sub>SC</sub> of 17 mA/cm<sup>2</sup> and V<sub>OC</sub> of 0.888 V. The charge separation and hole injection were studied by femtosecond laser.

In other work on solid-state sensitized perovskite solar cells,<sup>18</sup> the influence of the TiO<sub>2</sub> thickness and the perovskite concentration on the photovoltaic performance was investigated. The authors found that when the TiO<sub>2</sub> film is decreased there is more pore filling which results in an increase in the V<sub>OC</sub>; however, the optical density decreases. Figure 3 presents UV-vis spectra and current voltage curves of the cells at various perovskite concentrations and TiO<sub>2</sub> film thicknesses. The change in the photocurrent observed is due to charge collection efficiency rather than light absorption. The conclusion was the same as for the liquid perovskite cell – when using thin TiO<sub>2</sub> film (completely filling pores) the photovoltaic performance was improved.

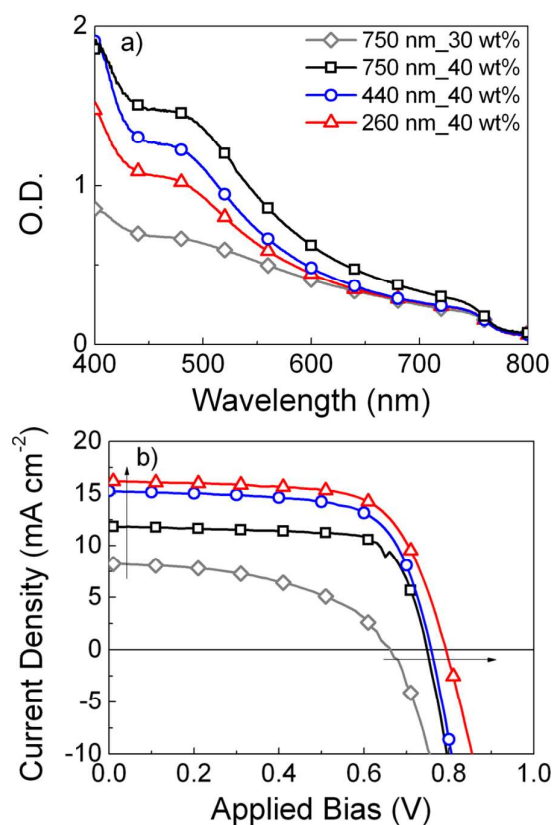


**Figure 3:** UV-vis spectroscopy and current density versus voltage curves of the solar cells. (a) UV-vis spectra of the relevant solar cells (before electrode deposition) with a 750 nm TiO<sub>2</sub> scaffold (m-TiO<sub>2</sub>) with 30 wt % perovskite precursor solution (gray diamonds), 750 nm TiO<sub>2</sub> with 40 wt % (black squares), 440 nm TiO<sub>2</sub> with 40 wt % (blue circles), 260 nm TiO<sub>2</sub> with 40 wt % (red triangles). These were taken in transmission mode in an integrating sphere to account for scattering. (b) Current density versus voltage curves of the same solar cells measured under 100 mW cm<sup>-2</sup> simulated AM1.5 solar irradiation. Taken from ref. 18 with permission.

Ogomi et al.<sup>19</sup> passivated the porous titania with Y<sub>2</sub>O<sub>3</sub> and with Al<sub>2</sub>O<sub>3</sub>. The passivation was done to remove surface traps of the porous titania to improve cells' efficiency. Measurements such as electron lifetime, thermally stimulated current, measurements of the microwave refractive carrier lifetime, and transient absorption spectroscopy were conducted. The authors show that surface passivation resulted in retardation of charge recombination between the electrons in the porous titania layers and the holes in the p-type organic conductors. Figure 4 shows longer recombination time for the passivated porous titania compared to a nonpassivated surface.

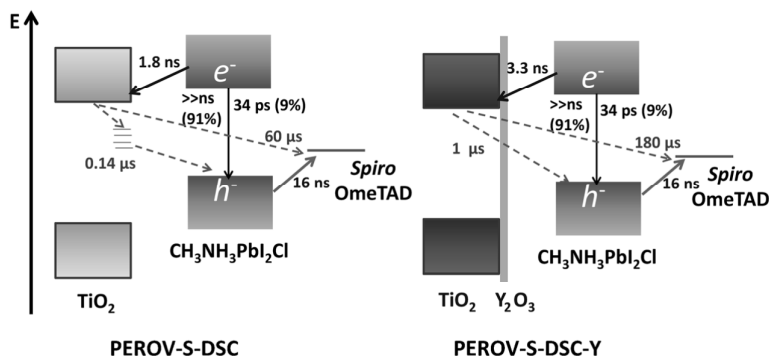


**Figure 4:** Carrier dynamics of perovskite-sensitized solar cell before and after  $\text{Y}_2\text{O}_3$  passivation. Taken with permission from ref. 19.

Sero and Bisquert et al.<sup>20</sup> used impedance spectroscopy to separate the physical parameters of carrier transport and recombination of two kinds of perovskite solar cells using different morphologies and compositions. The first perovskite was  $\text{CH}_3\text{NH}_3\text{PbI}_3$  with nanostructures of  $\text{TiO}_2$ , while the second cell was  $\text{CH}_3\text{NH}_3\text{PbI}_{3-x}\text{Cl}_x$  perovskite deposited on top of a compact thin film of  $\text{TiO}_2$ . In their study, both cells showed the same  $V_{oc}$ , although the FF,  $J_{sc}$  and the efficiency were higher for the thin film  $\text{TiO}_2$  cell.

Higher recombination rate was observed for the nanostructures of  $\text{TiO}_2$  although the transport rate and conductivity were similar for both cells, indicating that the perovskite is more efficient pathway for transport. (figure 5)

The authors determined the diffusion length for both cells using impedance spectroscopy. Both cells showed long diffusion length of around  $1 \mu\text{m}$ . In summary, the main difference between the morphologies, according to the interpretation of the impedance spectroscopy, is the higher recombination rate of the cells made with nanostructures of  $\text{TiO}_2$  film.

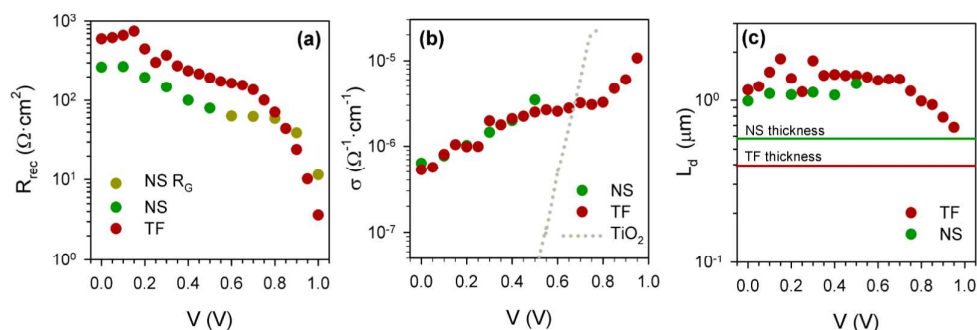


**Figure 5:** Transport and recombination parameters vs voltage: (a) recombination resistance,  $R_{rec}$ , (b) conductivity of active layer considering the geometric cell area, showing also the conductivity of nanostructured  $\text{TiO}_2$  in a DSC with spiro-MeOTAD hole conductor, and (c) diffusion length for NS and TF cells.  $R_{tr}$  and  $R_{rec}$  cannot be unambiguously defined when Gerischer pattern is observed (NS sample for  $V > 0.5$  V). Taken from ref. 20 with permission.

In addition to optical and electrochemical measurements, the structure of the perovskite after its deposition on the mesoporous metal oxide was investigated. Lindblad and Rensmoet et al.<sup>21</sup> measured the electronic structure and chemical composition of mesoporous  $\text{TiO}_2$  in  $\text{CH}_3\text{NH}_3\text{PbI}_3$  perovskite solar cells using hard X-ray photoelectron spectroscopy. The authors compared the one step deposition with the two step deposition and found similar stoichiometry and electronic structure. It was also shown that after perovskite deposition, the band gap states of  $\text{TiO}_2$  are still present.

A further study of the structure of  $\text{CH}_3\text{NH}_3\text{PbI}_3$  in mesoporous  $\text{TiO}_2$  was done by Choi and Owen et al.<sup>22</sup> using atomic pair distribution function (PDF) analysis of high energy X-ray diffraction data. Only 30% of the perovskite consists of medium range ordered crystalline, tetragonal perovskite, while the remaining 70% forms a highly disordered phase within the mesoporous  $\text{TiO}_2$  with short structural coherence of 1.4 nm. Moreover, the structure of the nano component was composed of small clusters of nanoparticles of two to eight octahedral lead iodide building blocks. The presence of disordered  $\text{CH}_3\text{NH}_3\text{PbI}_3$  strongly affects the photoluminescence (PL) spectra, which also affects the photovoltaic performance.

Edri and Cahen et al.<sup>23</sup> used electron beam-induced current (EBIC) imaging to study the cell mechanism of  $\text{CH}_3\text{NH}_3\text{PbI}_3$  and  $\text{CH}_3\text{NH}_3\text{PbI}_{3-x}\text{Cl}_x$ . They refer its structure to p-i-n devices. The authors extracted the diffusion length of electrons and holes from the EBIC contrast near the contacts (figure 6), and reveal that the diffusion length for holes is longer than the diffusion length for electrons with the former being at least

1  $\mu\text{m}$ . This finding is in disagreement with diffusion length of ca. 100 nm as deduced earlier.<sup>35,36</sup> (additional discussion about the diffusion length can be found in the next section) As a result, the  $\text{CH}_3\text{NH}_3\text{PbI}_3$  requires an electron conductor (mesoporous  $\text{TiO}_2$ ) because of the short diffusion length of the electrons. In contrast, due to the long diffusion length of the holes, hole-transporting material is not essential.

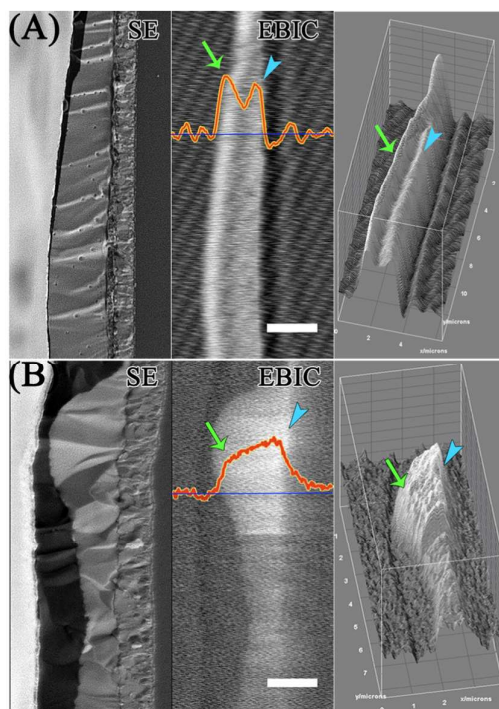


**Figure 6:** SE and EBIC images of cross sections of  $\text{CH}_3\text{NH}_3\text{PbI}_{3-x}\text{Cl}_x$  (A), scale bar is 2  $\mu\text{m}$ , and  $\text{CH}_3\text{NH}_3\text{PbI}_3$  (B), scale bar is 1  $\mu\text{m}$ , planar solar cells. Line scans were taken at the lines' positions. The arrows show the peaks for the I-Cl and where the peaks are in the case of the pure iodide. The right panel is a 3D surface plot of the EBIC images. The ripples observed in the EBIC image of (A) outside the (semi-)conductive regions are due to background noise. Taken from ref. 23 with permission.

#### 4. Planar perovskite based solar cells

An interesting and notable observation regarding perovskite-based solar cells is the ability to use them in planar architecture, which means that sensitized architecture isn't necessarily the only option for the perovskite to function in a solar cell. The planar architecture eliminates infiltration problems of the perovskite and the hole transport material into the porous, which results in less recombination and better reproducibility. Planar architecture opens the way to implementation of other deposition techniques, as will be described below. Figure 7 shows a schematic illustration

of the layers involved in the planar architecture.

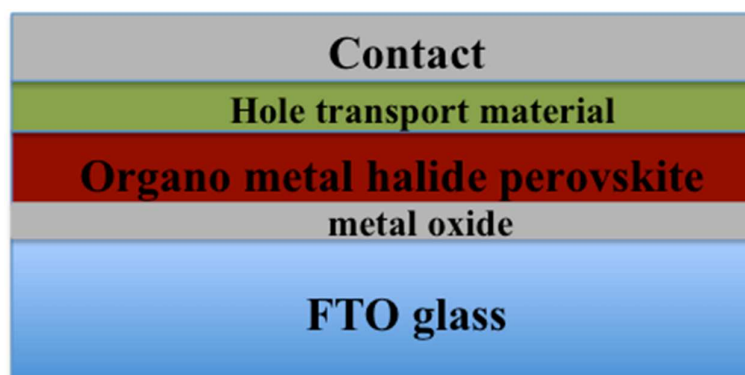


**Figure 7:** Schematic illustration of the planar heterojunction perovskite solar cell.

Lee and Snaith et al.<sup>24</sup> reported for the first time that the electron collector ( $\text{TiO}_2$  metal oxide) isn't necessary for the operation of the perovskite solar cells. In their study, they used photo induced absorption (PIA) spectroscopy to examine the charge separation at the mesoporous  $\text{TiO}_2$  and  $\text{Al}_2\text{O}_3$  coated with perovskite with and without HTM. In the  $\text{TiO}_2$  coated with perovskite, the PIA spectrum confirmed effective sensitization of the  $\text{TiO}_2$  by the perovskite. Alternatively,  $\text{Al}_2\text{O}_3$  coated with perovskite revealed no PIA signals, which confirmed the role of alumina as an insulator.

After adding the HTM, the oxidized species of the HTM (Spiro-OMETAD) created after photoexcitation of the perovskite were monitored. The research demonstrated that from the photoexcited perovskite to HTM the hole conductor is highly effective, and the hole transport material is necessary to enable long-lived charged species within the perovskite coated on  $\text{Al}_2\text{O}_3$ .

Moreover, small perturbation transient photocurrent decay measurements were performed to learn about the effectiveness of the perovskite as electronic charge transport. Charge collection in  $\text{Al}_2\text{O}_3$  based devices was faster by a factor of  $>10$  compared with  $\text{TiO}_2$  based devices, indicating that the electron diffusion through the perovskite is faster in  $\text{Al}_2\text{O}_3$  devices. The conclusion is that  $\text{Al}_2\text{O}_3$  is simply acting as a scaffold for the device, which means that the perovskite solar cell demonstrated in this work is not a sensitized solar cell. The authors refer the  $\text{Al}_2\text{O}_3$  cells as mesosuperstructured.

Low temperature planar perovskite solar cell was demonstrated using graphene flakes and presynthesized  $\text{TiO}_2$  nanoparticles.<sup>25</sup> The reported efficiency was 15.6%,

comparable to high temperature sintering process of  $\text{TiO}_2$  based devices. The graphene+ $\text{TiO}_2$  electrodes showed lower series resistance than the  $\text{TiO}_2$  electrodes; moreover, the recombination resistance was higher in the case of the graphene+ $\text{TiO}_2$  electrodes. The cross section of the device and its corresponding energy level diagram are presented in figure 8.

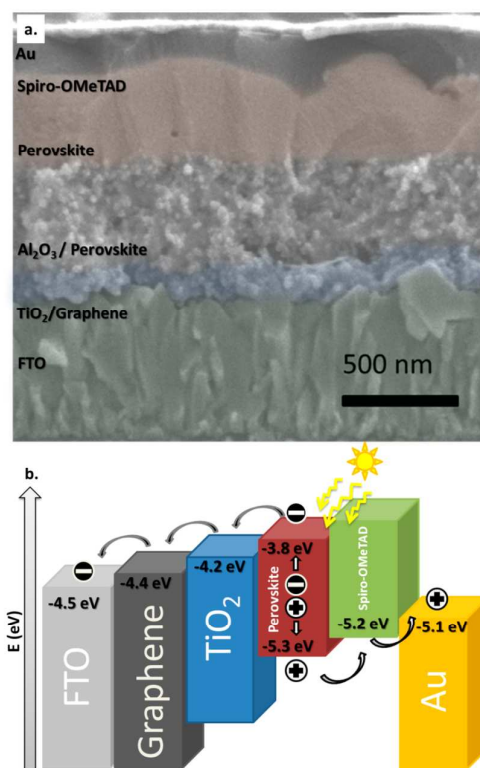


**Figure 8:** (a) Cross-sectional SEM shows the device structure. (b) Energy level diagram of the described low temperature device. The authors indicate that these are the energy levels of the individual materials, and upon contact within the solar cell, there is likely to be a considerable relative shift.<sup>26</sup> Authors added that the graphene and  $\text{TiO}_2$  were blended into a single composite layer and not layered as depicted in the energy level diagram. Taken from ref. 25 with permission.

Additional work on room temperature planar perovskite heterojunction solar cells was reported by using ZnO nanoparticles<sup>27</sup> as an alternative to both mesoporous  $\text{TiO}_2$  and  $\text{Al}_2\text{O}_3$  scaffolds. ZnO nanoparticles have a fabrication advantage due to the fact that they only need a spin coating step and do not require a heating and sintering step. Nanoparticles in the size range of 5 nm were made by hydrolysis of zinc acetate in methanol. Optimal film thickness was found to be around 25 nm and further increases in thickness did not improve PCE. The best PCE was found to be 15.7% with a 25 nm

film thickness which was achieved by doing three spin coating layers. The cells were prepared similarly to most planar heterojunction perovskite cells, where the perovskite was deposited on the ZnO layer; then the HTM layer was deposited on top of the perovskite. PCE of 10.2% was found when this fabrication technique was employed on a flexible substrate made of ITO/PET. A recent work on low temperature (sub 150<sup>0</sup>C) with meso-superstructured perovskite solar cells demonstrate slightly improved efficiency of 15.9%.<sup>28</sup>

The use of the planar architecture in flexible device was demonstrated<sup>29</sup> using CH<sub>3</sub>NH<sub>3</sub>PbI<sub>3-x</sub>Cl<sub>x</sub>, which was sandwiched between two organic contacts. The device structure employed (figure 9) was deemed “inverted” from regular device structure. The FTO was first coated with p-type material on top perovskite film, followed by n-type layer, finally aluminum was coated on top for the anode. Several p and n type contacts were studied. The best combination was PEDOT:PSS as the p-type layer and a bilayer of PCBM with a compact layer of TiOx as the n-type layer. The titanium was employed only to create a stable electrical contact with the anode. The power conversion achieved for this “inverted” structure was 9.8%, with optimal perovskite film thickness of 300–400 nm. The efficiency of this design was slightly lower than that of the regular cells structure due to a slightly lower FF.

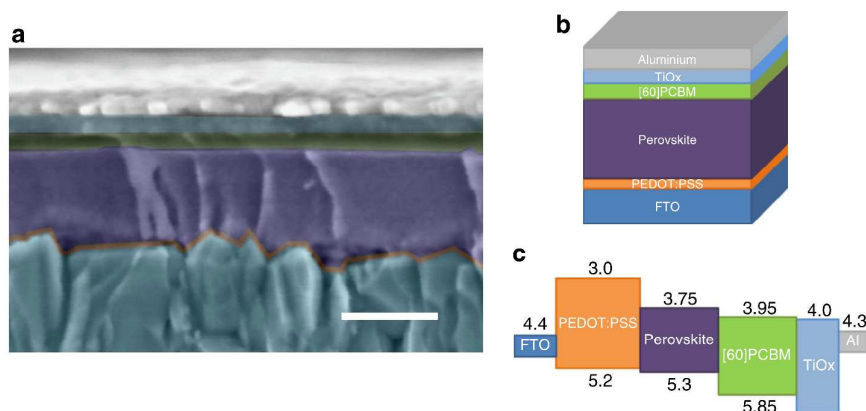


**Figure 9:** (a) Cross section of the inverted planar perovskite solar cell. Scale bar represents 250 nm. The different layers have been tinted with the color scheme of the device schematic shown in (b). (c) Approximate energy band diagram of the fabricated inverted structure taken from reference<sup>30</sup>. The figure was taken from ref. 29 with permission.

An interesting example for planar heterojunction perovskite solar cells is the ability to form semitransparent planar heterojunction solar cells with high efficiency.<sup>31</sup> Semitransparent solar cells can be integrated, for instance, into windows and automotive applications. In order to make semitransparent perovskite solar cells, it is essential to control the morphology of the perovskite thin film. One way to do that is to make perovskite “islands” which are small enough to appear continuous to the eye, but large enough to absorb the light to deliver high power conversion efficiency. The authors indicate that despite the observed voids in the films, high open circuit voltage and approximately 8% efficiency with 10% average of visible transmittance of the full device was observed.

As mentioned earlier one of the attractive properties of the perovskite is the ability to tune its optical properties by chemical modifications. One possible way to do it is to substitute the Pb with Sn, which results in an additional benefit, the reduction of the toxicity. Perovskite of the structure  $\text{CH}_3\text{NH}_3\text{Sn}_x\text{Pb}_{(1-x)}\text{I}_3$  was formed<sup>32</sup>, in which both the conduction and valence bands are shifted, and are shallower than those of titania by  $\sim -0.4\text{eV}$ . Power conversion efficiency of 4.18% was achieved for the perovskite having the chemical formula of  $\text{CH}_3\text{NH}_3\text{Sn}_{0.5}\text{Pb}_{0.5}\text{I}_3$ .

In this configuration, Spiro-OMETAD could not be successfully employed as an HTM due to having a HOMO level that was deeper than that of the perovskite. This made hole injection into the HTM difficult; therefore, P3HT was employed as an HTM instead. The IPCE curve shifted to 1060 nm in the best performing Sn-halide perovskite, compared to  $\text{CH}_3\text{NH}_3\text{PbI}_3$ , which has an IPCE edge of 800 nm. Figure 10 show the absorbance spectra of the several perovskite compositions.

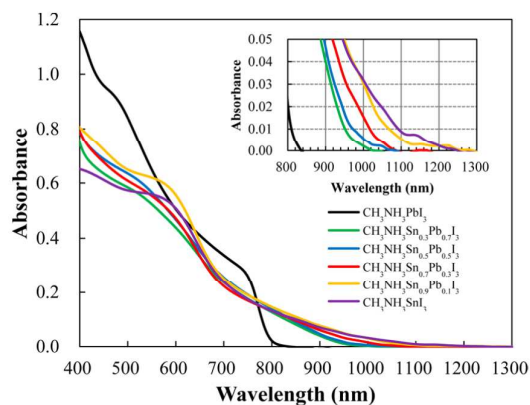


**Figure 10:** Absorption spectra of  $\text{CH}_3\text{NH}_3\text{Sn}_x\text{Pb}_{(1-x)}\text{I}_3$  perovskite coated on porous  $\text{TiO}_2$ . Taken from ref. 32 with permission.

Two recent reports showed complete substitution of the Pb by Sn which results with a lead free perovskite solar cell. In these reports the power conversion efficiency achieved was around 6%.<sup>33,34</sup>

The diffusion length of the electrons and holes was calculated<sup>35,36</sup> to be more than  $1\mu\text{m}$  for  $\text{CH}_3\text{NH}_3\text{PbI}_{3-x}\text{Cl}_x$ , justifying the high efficiency of the perovskite solar cell. As mentioned earlier different measurements techniques provide a variation in the calculated diffusion length, moreover the deposition technique also influence the diffusion length as indicated by Yang et al.<sup>43</sup> and Snaith et al.<sup>42</sup>. It is clear that long diffusion length of both carriers enables the use of the planar architecture.

The ability of perovskite to conduct both electrons and holes is an exceptional, distinctive property. This ability has been supported by the measurements of the long diffusion length of both carriers.<sup>35,36,20</sup> The ability to conduct both electrons and holes simplifies the device structure, enhancing the stability and eliminating the need to deal with infiltration issues of the HTM. The structure of the hole conductor free perovskite solar cell is presented in figure 11. Several research groups have already demonstrated enhanced PV performance of these hole conductor free perovskite solar cells, the highest PCE observed was 10.85%<sup>37,38,39,40</sup>. The current-voltage curve of the best PV performance is presented in figure 11B. Additionally, it appears that changing the halides in the perovskite (which influence its band gap) does not reduce its ability to conduct the electrons and holes as proved by its implementation in the hole conductor free devices.<sup>41</sup>

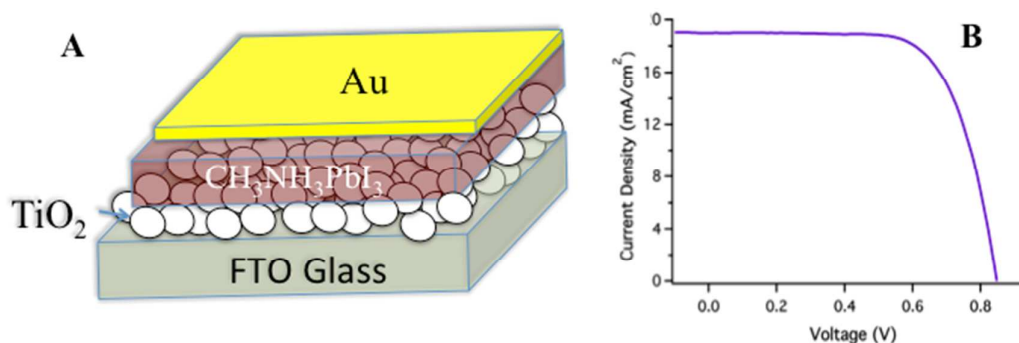


**Figure 11:**(A) The structure of the perovskite solar cells without a hole conductor. (B) Current voltage of the 10.8% efficiency for hole conductor free perovskite solar cells. Taken from ref. 38,39 with permission.

Vapor deposition technique was investigated for planar heterojunction perovskite solar cells achieving high efficiency.<sup>42</sup> A comparison between the vapor deposition

technique and the solution-processed technique was reported. For the vapor deposition technique, the film was stacked and uniform with a thickness of  $\sim 330$  nm. While for the solution-processed film, the thickness ranged between 50–410 nm and non-uniform. This is the explanation for the difference in performance; in the case of solution processed film, the voids in the perovskite layer lead to direct contact between the polymer and the  $\text{TiO}_2$  causing shunt path, that is, in part, responsible for lowering cell performance.

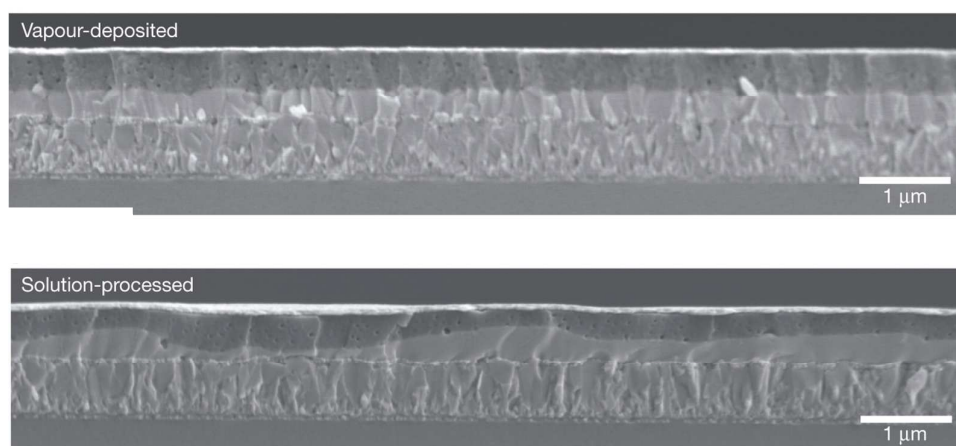


**Figure 12:** Cross section of devices made by the two different deposition techniques. Taken from ref. 42 with permission.

Except the vapor deposition technique mentioned, Chen and Yang et al.<sup>43</sup> demonstrate the use of the vapor assisted solution process (VASP) to fabricate the planar devices based on perovskite. This deposition technique requires the solution deposition of  $\text{PbI}_2$  with  $\text{CH}_3\text{NH}_3\text{I}$  vapor (see figure 13). The important point regarding the VASP technique is avoiding co-deposition of organic and inorganic species. Using this technique, the perovskite films are well defined with full surface coverage and low surface roughness that make them suitable for PV applications. Planar perovskite solar cells based on the VASP technique achieved PCE of 12.1%.

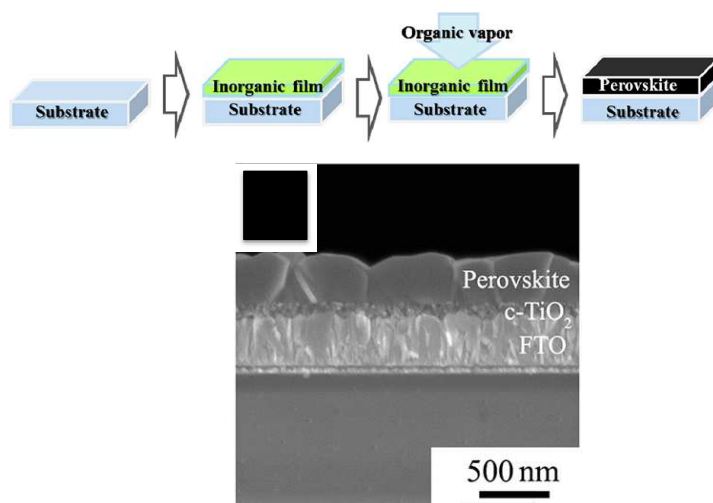


**Figure 13:** Scheme of the vapor assisted solution process (VASP) technique and SEM cross section of the planar perovskite based solar cell. Taken from ref. 43 with permission.

## 5. Summary and outlook

The fast growth of perovskite based solar cells in the recent years exhibits its potential to compete with the current technologies as a possible solution for solar energy.

Organo-metal halide perovskite has several advantages, making it an excellent candidate for use in photovoltaic solar cells. Its high absorption coefficient, optical band gap tuning, direct band gap, high stability, high carrier mobility, and the ability to use it in different device structures are important, even ideal, properties for a successful light harvester in a solar cell.

Further, perovskite does not require expensive and complicated techniques, but results from simple preparation, such as solution processed, spin coating or printing. In addition, the perovskite can be made under low temperature fabrication. These advantages position perovskite as a promising material for photovoltaic devices, superior to the current technologies—including organic PV, DSSC and even silicon solar cells.

Beyond these important properties, organo-metal halide perovskite isn't restricted to specific solar cell architecture. It can deliver high power conversion efficiencies in two main device structures, as described in this review—sensitized solar cell structure (originally came from the DSSC technology), and planar solar cell structure, indicated as thin film cells, or even in some cases, as extremely thin absorber cells. The following table summarizes the main points related to the architectures.

	<i>Sensitized architecture</i>	<i>Planar architecture</i>
<b>Operation mechanism</b>	Still not yet completely understood	Still not yet completely understood
<b>Electron-hole diffusion length</b>	Calculated to be the same for both architectures	Calculated to be the same for both architectures
<b>Solid hole transport material</b>	Used for both	Used for both
<b>Liquid electrolyte</b>	Used in this architecture	Not used
<b>Solution processed deposition techniques</b>	Used in this architecture	Used in this architecture
<b>Infiltration of perovskite and HTM</b>	Infiltration difficulties	No infiltration problems
<b>Recombination</b>	Higher recombination than the planar structure. The amount of pore filling determines the rate of recombination.	Less recombination than the sensitized architecture
<b>Metal oxide thickness</b>	Thicker metal oxide films	Thin metal oxide films
<b>Flexible devices</b>	Was not demonstrated yet	Used in this architecture
<b>Vapor deposition</b>	Not used	Used in this architecture
<b>Vapor-assisted solution processed technique-VLAP</b>	Not used	Used in this architecture
<b>Semitransparent devices</b>	Was not demonstrated yet	Used in this architecture

It can be said that organo-metal halide perovskite is a game changer in the solar energy technology. In just three years its efficiency increased more than 16%, 20% efficiency is just around the corner and 22%–23% efficiencies are attainable. Looking to the future, there are several ways to improve the perovskite-based solar cells. Perovskite deposition is a key issue to improve its coverage in order to achieve high efficiency cells. Tuning the band alignment between the different layers in the device could reduce energy losses and recombination. Increasing the charge density in the metal oxide film would improve charge separation and reduce the recombination rate. Finally, all device improvements should entail low cost techniques in keeping with the trend of the third generation cells. The ability to use perovskite in sensitized or planar architectures, in addition to its ambipolar properties, are definitely competitive advantages for achieving high power conversion efficiencies.

## 6. References

- <sup>1</sup> Akihiro Kojima; Kenjiro Teshima; Yasuo Shirai; Tsutomu Miyasaka. Organometal Halide Perovskites as Visible-Light Sensitizers for Photovoltaic Cells. *J. Am. Chem. Soc.* **2009**, 131, 6050–6051.
- <sup>2</sup> [http://www.nrel.gov/ncpv/images/efficiency\\_chart.jpg](http://www.nrel.gov/ncpv/images/efficiency_chart.jpg)
- <sup>3</sup> Julian Burschka, Norman Pellet, Soo-Jin Moon, Robin Humphry-Baker, Peng Gao, Mohammad K. Nazeeruddin & Michael Graetzel, *Nature*, **2013**, 499, 316.
- <sup>4</sup> J. T.-W. Wang, J. M. Ball, E. M. Barea, A. Abate, J. A. Alexander-Webber, J. Huang, M. Saliba, I. Mora-Sero, J. Bisquert, H.J. Snaith, R. J. Nicholas, *Nano Lett.*, 2014, 14, 724.
- <sup>5</sup> Nam Joong Jeon, Hag Geun Lee, Young Chan Kim, Jangwon Seo, Jun Hong Noh, Jaemin Lee, and Sang Il Seok, o-Methoxy Substituents in Spiro-OMeTAD for Efficient Inorganic–Organic Hybrid Perovskite Solar Cells *J. Am. Chem. Soc.*, **2014**, 136 (22), 7837–7840.
- <sup>6</sup> Bing Cai, Yedi Xing, Zhou Yang, Wen-Hua Zhang and Jieshan Qiu, High performance hybrid solar cells sensitized by organolead halide perovskites, *Energy Environ. Sci.*, **2013**, 6, 1480.
- <sup>7</sup> Eran Edri, Saar Kirmayer, David Cahen, and Gary Hodes, High Open-Circuit Voltage Solar Cells Based on Organic–Inorganic Lead Bromide Perovskite, *J. Phys. Chem. Lett.* **2013**, DOI: 10.1021/jz400348q.
- <sup>8</sup> A.S. Bhalla, R. Guo and R. Roy, The perovskite structure – a review of its role in ceramic science and technology, *Mat. Res. Innovat.* **4**, 3-26 (2000) and references therein.
- <sup>9</sup> Mitzi, D. B. Synthesis, Structure, and Properties of Organic–Inorganic Perovskites and Related Materials, in *Progress in Inorganic Chemistry*, 1999, 48, John Wiley & Sons, Inc., New York, p. 1.
- <sup>10</sup> Giles E. Eperon, Samuel D. Stranks, Christopher Menelaou, Michael B. Johnston, Laura M. Herz and Henry J. Snaith, Formamidinium lead trihalide: a broadly tunable perovskite for efficient planar heterojunction solar cells, *Energy Environ. Sci.*, **2014**, 7, 982-988.
- <sup>11</sup> Noh, J. H., Im, S. H., Heo, J. H., Mandal, T. N. & Seok, S. I. Chemical management for colorful, efficient, and stable inorganic–organic hybrid nanostructured solar cells. *Nano Lett.* **2013**, 13, 1764–1769.
- <sup>12</sup> Kojima, A.; Ikegami, M.; Teshima, K.; Miyasaka, T. Highly Luminescent Lead Bromide Perovskite Nanoparticles Synthesized with Porous Alumina Media. *Chem. Lett.* **2012**, 41, 397.
- <sup>13</sup> Kagan, C. R.; D. Mitzi, B.; Dimitrakopoulos, C. D. Organic-Inorganic Hybrid Materials as Semiconducting Channels in Thin-Film Field-Effect Transistors. *Science*, **1999**, 286, 945.
- <sup>14</sup> Mitzi, D. B.; Field, C. A.; Schlesinger, Z.; Laibowitz, R. B. Transport Optical and Magnetic properties of the conducting Halide Perovskite  $\text{CH}_3\text{NH}_3\text{SnI}_3$ . *J. Solid State Chem.* **1995**, 114, 159.
- <sup>15</sup> Im JH, Lee CR, Lee JW, Park SW, Park NG. 6.5% efficient perovskite quantum-dot-sensitized solar cell. *Nanoscale*. **2011**, 3(10):4088-93.
- <sup>16</sup> Yixin Zhao and Kai Zhu, Charge Transport and Recombination in Perovskite  $(\text{CH}_3\text{NH}_3)\text{PbI}_3$  Sensitized  $\text{TiO}_2$  Solar Cells. *J. Phys. Chem. Lett.* **2013**, 4, 2880–2884.
- <sup>17</sup> Hui-Seon Kim, Chang-Ryul Lee, Jeong-Hyeok Im, Ki-Beom Lee, Thomas Moehl,

Arianna Marchioro, Soo-Jin Moon, Robin Humphry-Baker, Jun-Ho Yum, Jacques E. Moser, Michael Grätzel, Nam-Gyu Park, Lead Iodide Perovskite Sensitized All-Solid-State Submicron Thin Film Mesoscopic Solar Cell with Efficiency Exceeding 9%. *Nature Scientific Reports*, **2013**, 591 doi:10.1038/srep00591.

<sup>18</sup> Tomas Leijtens, Beat Lauber, Giles E. Eperon, Samuel D. Stranks, and Henry J. Snaith, The Importance of Perovskite Pore Filling in Organometal Mixed Halide Sensitized TiO<sub>2</sub> Based Solar Cells. *J. Phys. Chem. Lett.* **2014**, *5*, 1096–1102.

<sup>19</sup> Yuhei Ogomi, Kenji Kukihara, Shen Qing, Taro Toyoda, Kenji Yoshino, Shyam Pandey, Hisayo Momose, and Shuzi Hayase, Control of Charge Dynamics through a Charge-Separation Interface for All-Solid Perovskite-Sensitized Solar Cells. *Chem Phys Chem*, **2013**, DOI: 10.1002/cphc.201301153.

<sup>20</sup> Victoria Gonzalez-Pedro, Emilio J. Juarez-Perez, Waode-Sukmawati Arsyad, Eva M. Barea, Francisco Fabregat-Santiago, Ivan Mora-Sero, and Juan Bisquert, General Working Principles of CH<sub>3</sub>NH<sub>3</sub>PbX<sub>3</sub> Perovskite Solar Cells. *Nano Lett.* **2014**, *14*, 888–893.

<sup>21</sup> Rebecka Lindblad, Dongqin Bi, Byung-wook Park, Johan Oscarsson, Mihaela Gorgoi, Hans Siegbahn, Michael Odellius, Erik M. J. Johansson, and Håkan Rensmo, Electronic Structure of TiO<sub>2</sub>/CH<sub>3</sub>NH<sub>3</sub>PbI<sub>3</sub> Perovskite Solar Cell Interfaces. *J. Phys. Chem. Lett.* **2014**, *5*, 648–653.

<sup>22</sup> Joshua J. Choi, Xiaohao Yang, Zachariah M. Norman, Simon J. L. Billinge, and Jonathan S. Owen, Structure of Methylammonium Lead Iodide Within Mesoporous Titanium Dioxide: Active Material in High-Performance Perovskite Solar Cells. *Nano Lett.* **2014**, *14*, 127–133.

<sup>23</sup> Eran Edri, Saar Kirmayer, Alex Henning, Sabyasachi Mukhopadhyay, Konstantin Gartsman, Yossi Rosenwaks, Gary Hodes, and David Cahen, Why Lead Methylammonium Tri-Iodide Perovskite-Based Solar Cells Require a Mesoporous Electron Transporting Scaffold (but Not Necessarily a Hole Conductor). *Nano Lett.* **2014**, *14*, 1000–1004.

<sup>24</sup> Michael M. Lee, Joël Teuscher, Tsutomu Miyasaka, Takuro N. Murakami, Henry J. Snaith, Efficient Hybrid Solar Cells Based on Meso-Superstructured Organometal Halide Perovskites. *Science*, **2012**, *338*, 643–647.

<sup>25</sup> Jacob Tse-Wei Wang, James M. Ball, Eva M. Barea, Antonio Abate, Jack A. Alexander-Webber, Jian Huang, Michael Saliba, Ivan À Mora-Sero, Juan Bisquert, Henry J. Snaith, and Robin J. Nicholas, Low-Temperature Processed Electron Collection Layers of Graphene/ TiO<sub>2</sub> Nanocomposites in Thin Film Perovskite Solar Cells. *Nano Lett.* **2014**, *14*, 724–730.

<sup>26</sup> Wang, X.; Zhi, L.; Muellen, K. *Nano Lett.* **2008**, *8* (1), 323–327.

<sup>27</sup> Dianyí Liu and Timothy L. Kelly, Perovskite solar cells with a planar heterojunction structure prepared using room-temperature solution processing techniques. *Nature photonics*, **2014**, *8*, 133–138.

<sup>28</sup> Konrad Wojciechowski, Michael Saliba, Tomas Leijtens, Antonio Abate and Henry J. Snaith, Sub-150C processed meso-superstructured perovskite solar cells with enhanced efficiency, *Energy Environ. Sci.*, **2014**, *7*, 1142.

<sup>29</sup> Pablo Docampo, James M. Ball, Mariam Darwich, Giles E. Eperon Henry J. Snaith, Efficient organometal trihalide perovskite planar-heterojunction solar cells on flexible polymer substrates. *Nature Comm.*, **2013**, DOI: 10.1038/ncomms3761.

<sup>30</sup> Abrusci, A. et al. High performance perovskite-polymer hybrid solar cells via electronic coupling with fullerene monolayers. *Nano Lett.* **2013**, *13*, 3124–3128.

<sup>31</sup> Giles E. Eperon, Victor M. Burlakov, Alain Goriely, and Henry J. Snaith, Neutral

Color Semitransparent Microstructured Perovskite Solar Cells. *ACS Nano*, **2014**, 8, 591-598.

<sup>32</sup> Yuhei Ogomi, Atsushi Morita, Syota Tsukamoto, Takahiro Saitho, Naotaka Fujikawa, Qing Shen, Taro Toyoda, Kenji Yoshino, Shyam S. Pandey, Tingli Ma, and Shuzi Hayase,  $\text{CH}_3\text{NH}_3\text{Sn}_x\text{Pb}_{(1-x)}\text{I}_3$  Perovskite Solar Cells Covering up to 1060 nm. *J. Phys. Chem. Lett.* **2014**, 5, 1004-1011.

<sup>33</sup> Nakita K. Noel, Samuel D. Stranks, Antonio Abate, Christian Wehrenfennig, Simone Guarnera, Amir Haghighirad, Aditya Sadhanala, Giles E Eperon, Sandeep K. Pathak, Michael B Johnston, annamaria petrozza, Laura Herz and Henry Snaith, Lead-Free Organic-Inorganic Tin Halide Perovskites for Photovoltaic Applications, *Energy Environ. Sci.*, **2014**, DOI: 10.1039/C4EE01076K.

<sup>34</sup> Feng Hao, Constantinos C. Stoumpos, Duyen Hanh Cao, Robert P. H. Chang and Mercouri G. Kanatzidis, Lead-free solid-state organic-inorganic halide perovskite solar cells, *Nature photonic*, **2014**, 8, 489.

<sup>35</sup> Guichuan Xing, Nripan Mathews, Shuangyong Sun, Swee Sien Lim, Yeng Ming Lam, Michael Grätzel, Subodh Mhaisalkar, Tze Chien Sum, Long-Range Balanced Electron- and Hole-Transport Lengths in Organic-Inorganic  $\text{CH}_3\text{NH}_3\text{PbI}_3$ . *Science*, **2013**, 342, 344.

<sup>36</sup> Samuel D. Stranks, Giles E. Eperon, Giulia Grancini, Christopher Menelaou, Marcelo J. P. Alcocer, Tomas Leijtens, Laura M. Herz, Annamaria Petrozza, Henry J. Snaith, Electron-Hole Diffusion Lengths Exceeding 1 Micrometer in an Organometal Trihalide Perovskite Absorber. *Science*, **2013**, 342, 34-344.

<sup>37</sup> Jiangjian Shi, Juan Dong, Songtao Lv, Yuzhuan Xu, Lifeng Zhu, Junyan Xiao, Xin Xu, Huijue Wu, Dongmei Li, Yanhong Luo and Qingbo Meng, Hole-conductor-free perovskite organic lead iodide heterojunction thin-film solar cells: High efficiency and junction property. *Appl. Phys. Lett.* **2014**, 104, 063901.

<sup>38</sup> Sigalit Aharon, Shany Gamliel, Bat El Cohen and Lioz Etgar, Depletion region effect of highly efficient hole conductor free  $\text{CH}_3\text{NH}_3\text{PbI}_3$  perovskite solar cells. *Phys. Chem. Chem. Phys.*, **2014**, DOI: 10.1039/C4CP00460D.

<sup>39</sup> Waleed Abu Labana and Lioz Etgar, Depleted hole conductor-free lead halide iodide heterojunction solar cells. *Energy Environ. Sci.*, 2013, 6, 3249-3253.

<sup>40</sup> Lioz Etgar, Peng Gao, Zhaosheng Xue, Qin Peng, Aravind Kumar Chandiran, Bin Liu, Md. K. Nazeeruddin, and Michael Grätzel, Mesoscopic  $\text{CH}_3\text{NH}_3\text{PbI}_3/\text{TiO}_2$  Heterojunction Solar Cells. *J. Am. Chem. Soc.*, **2012**, 134 (42), 17396–17399.

<sup>41</sup> Sigalit Aharon, Bat-El Cohen, and Lioz Etgar, Hybrid Lead Halide Iodide and Lead Halide Bromide in Efficient Hole Conductor Free Perovskite Solar Cell. *J. Phys. Chem. C*, **2014**, DOI: 10.1021/jp5023407.

<sup>42</sup> Mingzhen Liu, Michael B. Johnston & Henry J. Snaith, Efficient planar heterojunction perovskite solar cells by vapour deposition. *Nature*, **2013**, 501, 395-399.

<sup>43</sup> Qi Chen, Huanping Zhou, Ziruo Hong, Song Luo, Hsin-Sheng Duan, Hsin-Hua Wang, Yongsheng Liu, Gang Li, and Yang Yang, Planar Heterojunction Perovskite Solar Cells via Vapor-Assisted Solution Process. *J. Am. Chem. Soc.* **2014**, 136, 622-625.

**TOC**

This review describes studies in the field of perovskite solar cells comparing two solar cell architectures sensitized versus planar structure.

